Nonresonance Raman Study of the Flavin Cofactor and Its Interactions in the Methylotrophic Bacterium W3A1 Electron-Transfer Flavoprotein

Kun-Yun Yang[‡] and Richard P. Swenson*[,‡,§]

Biophysics Program and Department of Biochemistry, The Ohio State University, Columbus, Ohio 43210

Received August 10, 2006; Revised Manuscript Received December 19, 2006

ABSTRACT: Nonresonance Raman spectroscopy has been used to investigate the protein−flavin interactions of the oxidized and anionic semiquinone states of the electron-transfer flavoprotein from the methylotrophic bacteria W3A1 (wETF) in solution. Several unique features of oxidized wETF were revealed from the Raman data. The unusually high frequency of the Raman band for the C(4)═O of the flavin suggests that hydrogen-bonding interactions with the C(4)O are very weak or nonexistent in wETF. In contrast, hydrogen bonding with the C(2)═O is one of the strongest among the flavoproteins investigated thus far. According to the crystal structure, the side-chain hydroxyl group of αSer254 serves as a hydrogen bond donor to the N(5) atom in the oxidized flavin cofactor in wETF. The replacement of αSer254 by cysteine by site-directed mutagenesis resulted in shifts in N(5)-relevant Raman bands in both the oxidized and anionic semiquinone states of the protein. These results confirm the presence of the hydrogen-bonding interaction at N(5) that is evident in the crystal structure of the oxidized protein and that it persists in the one-electron reduced state. The data suggest that these bands can serve as useful Raman markers for the N(5) interactions in both oxidation states of flavoproteins. The wETF displays unusually low frequencies of flavin ring I (*o*-xylene ring) relevant bands, which suggests a ring I microenvironment different from most of the other flavoproteins. As indicated by Raman data, the αS254C mutation changed the environment of ring I, perhaps as the consequence of changes in the mobility of the FAD domain of wETF. These unusual flavin−protein interactions may be associated with the unique redox properties of wETF.

Electron-transfer flavoproteins (ETFs) are a family of flavoproteins that mediate the transfer of electrons from a variety of degradative dehydrogenases to membrane-bound electron acceptors in mitochondria and bacteria (*1*). With the exception of the ETF from *Megasphera elsdenii*, which contains 2 equiv of FAD[1] (*2*), all other ETFs contain 1 equiv of noncovalently bound FAD as their redox cofactor. Under physiological conditions, the FAD cycles between the oxidized (OX) and the anionic semiquinone (SQ) states. Further reduction of the ETF by dehydrogenases appears not to be kinetically significant (*1*). Sequence comparisons among all ETFs and ETF-like proteins reveal the existence of two distinguishable subfamilies (*3*). Group I includes the "housekeeping" ETFs that link degradative dehydrogenase reactions with the respiratory electron transport chain, such as in the fatty acid degradation pathway. Human ETF (hETF) and other mammalian ETFs belong to this group. The defects in hETF or its electron acceptor result in glutaric acidemia type II (GAII), an often fatal genetic metabolic disease resulting from the failure to catabolize various fatty acyl-CoAs (*4*). Group II contains ETF-like proteins that are synthesized only under certain growth conditions and receive electrons from the oxidation of specific substrates. As a typical example of this group, the more extensively studied ETF from the methylotrophic bacteria W3A1 (wETF) serves as the physiological electron acceptor for trimethylamine dehydrogenase (*5*). wETF has several unique properties including a midpoint potential for the first couple that is the highest among all the flavoproteins (*6*). The SQ is also unusually stable in this protein, being resistant to air reoxidation, but more so to further reduction to the hydroquinone (HQ) state (*6*).

Knowledge of the structural basis of these properties is critical in our understanding of the electron-transfer mechanism of this family as well as generally how flavoproteins modulate the physical and chemical properties of the flavin cofactor to facilitate their biological functions. The specific flavin−protein interactions in wETF can be deduced from its crystal structure (*7*). However, such structural information may reflect only the conformational state of the protein in the crystal. ETF proteins seem to demonstrate a high level of conformational flexibility in solution (*7*). In addition, the SQ state of flavins, a crucial intermediate in redox and electron-transfer reactions of most flavoproteins, is often technically difficult to study because of its intrinsic instability. Thus, various types of spectroscopy can provide a more direct and convenient way to evaluate such interactions under solution conditions more comparable to the physiological conditions under which most biochemical data have been obtained. NMR has been applied to study the flavin−protein

* To whom correspondence should be addressed. Tel: 614-292-9428. Fax: 614-292-6773. E-mail: swenson.1@osu.edu.

[‡] Biophysics Program.

[§] Department of Biochemistry.

[1] Abbreviations: FAD, flavin adenine dinucleotide; wETF, hETF, and pETF, electron-transfer flavoprotein from methylotrophic bacterium W3A1, human, and *Paracoccus denitrificans*, respectively; OX, SQ, and HQ, the oxidized, semiquinone, and hydroquinone states of the flavin cofactor.

10.1021/bi061628a CCC: $37.00
Published on Web 02/10/2007

interactions in the oxidized or fully reduced HQ states in various flavoproteins, including hETF (*8*). However, the SQ state, a paramagnetic species, is still inaccessible using NMR approaches.

Raman spectroscopy, which provides vibrational information for chemical bonds, is particularly sensitive to the changes in the chemical environment of relevant atoms. The assignments of the various Raman bands of oxidized flavins have been established by theoretical calculations (*9*−*14*) and experimental isotopic substitutions of flavins (*11*). Raman spectroscopy has been successfully applied to evaluate important flavin−protein interactions in various oxidized flavoproteins (*12*−*15*). The Raman spectra for the anionic SQ form (SQ^-) of bound or free flavins have also been reported previously (*16*−*20*). However, this approach has rarely been applied to study the interactions of the SQ^- form of the flavin with apoprotein in flavoproteins. The intrinsic instability of the flavin SQ^- is one of the obstacles for obtaining high-quality Raman spectra. In some published Raman studies on this redox state, the flavin SQ^- had to be stabilized by adding high concentrations of substrate analogues under anaerobic conditions (*16*, *19*) or technically difficult time-resolved techniques were required (*17*, *18*).

In this work, enhanced nonresonance Raman spectroscopy (*14*, *21*) was effectively utilized to investigate several specific flavin−protein interactions in both the OX and the SQ^- states of the flavin cofactor within the same flavoprotein, in this case wETF, which displays unusual redox and electron-transferring properties. This approach has the advantage over more frequently used resonance Raman spectroscopy in substantially reducing the high fluorescence background, overheating, and laser-induced photodegradation of flavoprotein samples. The exceptional stability of the SQ^- form of wETF permitted the acquisition of high-quality nonresonance Raman spectra of the flavin SQ^- state. With the aid of the crystallographic structural information and site-directed mutagenesis, Raman spectral changes associated with alterations in the N(5) hydrogen-bonding interaction in the OX and SQ^- states were evaluated in this study as reference markers of this interactions in other flavoproteins. The Raman data also provided evidence for protein dynamics that alter the environment of the *o*-xylene portion of the flavin. Conformational changes have been implicated in the electron-transfer mechanism of the protein (*7*).

MATERIALS AND METHODS

Protein Sample Preparation. The recombinant wild-type wETF protein and its αS254C mutant were prepared and expressed in *Escherichia coli* cells (strain JM105) and purified as described previously (*22*). Apoprotein was prepared by extensive dialysis of the holoprotein against 50 mM potassium phosphate buffer, pH 7.2, containing 0.3 mM EDTA and 2.0 M KBr, followed by dialysis against the phosphate−EDTA buffer to remove the KBr. Samples of the wETF in the anionic SQ state were prepared just prior to spectroscopic analysis by the addition of sodium dithionite solution to a final concentration of 2 mM. Samples remained reduced throughout the Raman data acquisition as confirmed postanalysis by UV−visible spectroscopy.

Raman Spectroscopy. Each Raman spectrum for the bound FAD was obtained by subtraction of the Raman spectrum of apoETF from that of holoETF, both of which were acquired under identical conditions using nonresonance infrared laser excitation at 752 nm as previously described (*14*, *21*).

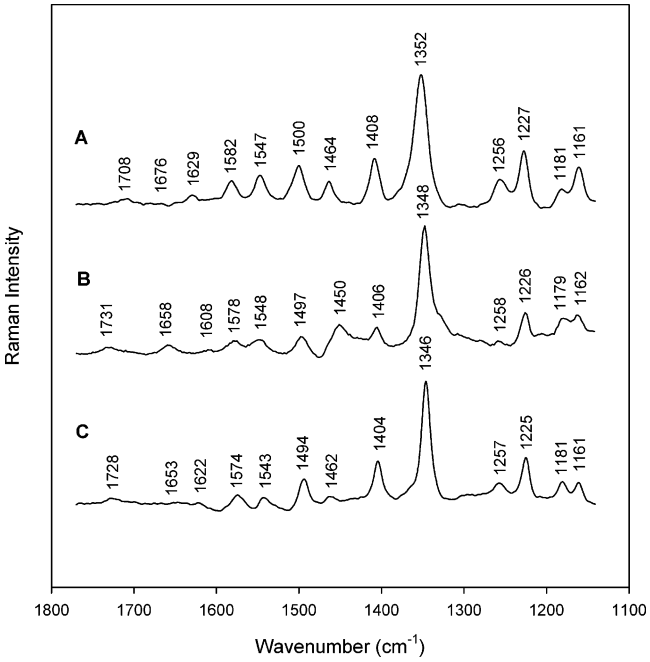

FIGURE 1: Raman spectra of FAD (A), wild-type wETF (B), and wETF αS254C mutant (C). The sample concentrations were 200 μM in 50 mM phosphate buffer, pH 7.2, 25 °C. Data were collected at 752 nm at 1.1 W of laser excitation with 10 min binning as previously described (*14*, *21*).

Table 1: Frequencies (cm^{-1}) of Raman Bands of Oxidized Free FAD, wETF-WT, and wETF αS254C Mutant

band[a]	FAD	wETF-WT	wETF-αS254C
C4═O	1708	1731	1728
C2═O	1676	1658	1653
I	1629	1608	1622
II	1582	1578	1574
III	1547	1548	1543
IV	1500	1497	1494
V	1464	1450	1462
VI	1408	1406	1404
VII	1352	1348	1346
X	1256	1258	1257
XI	1227	1226	1225
XII	1181	1179	1181
XIII	1161	1162	1161

[a] Band numbering according to Bowman and Spiro (*9*).

RESULTS AND DISCUSSION

Raman Spectra of Oxidized wETF Wild-Type and αS254C Mutant. The Raman spectra in the high-frequency region for oxidized FAD in solution and when bound to the wild-type wETF and its αS254C mutant (Figure 1) reveal a set of typical flavin Raman bands that are consistent with published spectra of oxidized flavins (*14*, *21*, *23*). The Raman shifts for each sample are summarized in Table 1 using the flavin Raman band numbering system of Bowman and Spiro (*9*) and in Figure 2, which shows the differences between the band frequencies of free and bound FAD in the wild-type and the mutant wETF. Significant frequency shifts were observed in the region above 1500 cm^{-1}. Especially noteworthy were the relatively large frequency shifts observed

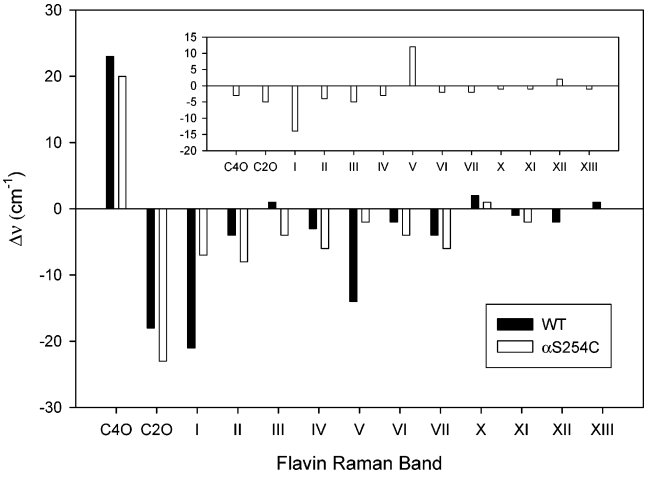

FIGURE 2: Frequency changes of flavin Raman bands for wild-type wETF and wETF αS254C mutant relative to free FAD. Inset: Frequency differences between wild-type wETF and wETF αS254C mutant.

for the C(4)═O and C(2)═O bands and bands I and V, which shift by up to 20 cm^{-1} in wild-type and αS254C mutant proteins when compared with the unbound FAD and by 3−14 cm^{-1} when the mutant is compared to the wild-type protein (Figure 2 inset).

Environments of the Flavin C(4)O and C(2)O Groups in wETF. According to previous assignments established by isotopic substitutions and theoretical calculations (*9*−*14*, *24*, *25*), the flavin Raman band around 1710 cm^{-1} is associated nearly exclusively with the carbonyl stretching mode of the C(4)═O. The frequency of this band correlates linearly with the chemical shift of the carbonyl carbon (*24*), the bond length, and the enthalpy of the H-bond on carbonyl oxygen (*26*), all of which are reflective of changes in the electron density of the carbonyl group. The lower frequency of this band correlates with a strong hydrogen-bonding interaction with the carbonyl moiety (*11*, *24*, *25*). In the wild-type wETF, the observed frequency of 1731 cm^{-1} represents the highest value thus far observed for the C(4)═O stretching mode in oxidized flavins. The C(4)═O group points toward the center of a reverse turn in the wETF protein. Several heteroatoms are within 3.5 Å of the C(4)O, including the backbone amide NH groups of αSer254 (3.0 Å) and αGln253 (3.2 Å) as well as the hydroxyl group of αSer254 (3.3 Å) and possibly the side-chain carbonyl group of αGln250 (2.9 Å) (PDB code, 1O97) (*7*). The high frequency of the C(4)═O suggests that this environment may not favor the formation strong H-bonds with the C(4)O in this protein. It is also possible that the frequency of the carbonyl may be influenced by unfavorable dipolar interactions. In fact, the substitution of αSer254 with a cysteine residue, which has both a weaker hydrogen-bonding potential and a lower dipole moment than the hydroxyl group of serine, decreased slightly the frequency of C(4)═O band relative to wild type (see Figures 1 and 2). A similar environment for the C(4)═O is apparent in the crystal structure of hETF. Although Raman data are not available for hETF, a C(4)═O stretching frequency of 1724 cm^{-1} can be estimated from the NMR ^{13}C chemical shift value of 162.3 ppm for the $^{13}C(4)$ in this protein (*8*) using the empirical linear relationship of Hazekawa et al. for this carbonyl moiety, where δ (ppm) = 429.48 − 0.155 × (Raman shift) (cm^{-1}) (*24*). Conversely, a chemical shift value for the $^{13}C(4)$ of 161.2 ppm can be calculated for wETF based on the observed Raman frequency of 1731 cm^{-1}. These represent the highest chemical shift values for any $^{13}C(4)$ atom observed in all the flavins or flavoproteins investigated thus far. Riboflavin binding protein also displays a Raman band for the C(4)═O that is quite high (1723 cm^{-1}) (*25*). H-bonding interactions with the C(4)═O of riboflavin are not apparent in the crystal structure of this protein, with the closest protein atoms to the C(4)O being 4.8 Å (*27*). Thus, our Raman results suggest that the C(4)═O of the FAD may not be hydrogen bonded to the wETF and hETF proteins in the oxidized state.

The stretching mode for the C(2)═O also contributes to a carbonyl Raman band at a frequency around 1665 cm^{-1}. Because of its weak intensity, the C(2)═O Raman band of flavin has not been studied experimentally in detail. The frequency of the C(2)═O band in wETF is substantially lower than for free FAD in solution (1658 versus 1676 cm^{-1}, respectively) and is also lower than most of C(2)═O frequencies observed thus far in flavoproteins. Similarly, the NMR chemical shift value of 161.0 ppm reported for the $^{13}C(2)$ in hETF is one of the highest in investigated flavoproteins, second only to that of flavocytochrome b2 (161.5 ppm) (*28*). By these criteria, the hydrogen-bonding interactions at the C(2)O in wETF and hETF may be among the strongest within flavoproteins. An extensive hydrogen-bonding network to the C(2)O is noted in these proteins. For wETF, this network involves the Nδ of αHis275 (2.9 Å), the backbone amide group of αArg237 (2.9 Å), and the O′ (4) of ribityl side chain of the FAD itself (3.2 Å) (PDB code, 1O97) (*7*) (Figure 3B). A similar network is found in hETF (PDB code, 1EFV) (*29*), although somewhat longer apparent donor/acceptor distances are noted (Figure 3A). These H-bond network and short donor−acceptor distances also imply that the C(2)O is involved in strong hydrogen-bonding interactions in both proteins.

The role of the hydrogen-bonding interactions with the carbonyl groups of flavin cofactor in establishing the properties of flavoproteins has rarely been studied systematically. For glycolate oxidase (*28*) and old yellow enzyme (*30*), changes in the hydrogen bonding at C(4)O induced by site-directed amino acid replacements can significantly influence the redox potential, the stability of SQ state, and other catalytic properties of the protein-bound flavins. Thus far, there lacks experimental study on the effects of C(2)O hydrogen-bonding interactions on the properties of the flavin cofactor in flavoproteins. The strong C(2)O hydrogen-bonding interactions in wETF, as indicated by our Raman data, could thermodynamically stabilize SQ^- state of the FAD because the negative charge of this redox state is localized in the N(1)−C(2)═O region of the flavin (*31*). In addition, this interaction could substantially affect the overall dipole moment of the flavin isoalloxazine ring because the two carbonyl groups contribute substantially to its polarity (*32*). Thus, interactions with the carbonyl groups of the flavin may very well be one of the structural determinants for the extraordinarily high midpoint potential for the OX/SQ couple and the remarkable stability of the SQ^- state of this protein.

Establishing a Raman Marker for N(5) Hydrogen-Bonding Interaction in the Oxidized State of wETF. Raman spectroscopy also provides a potential method for evaluating hydrogen-bonding interactions at the N(5) position of the

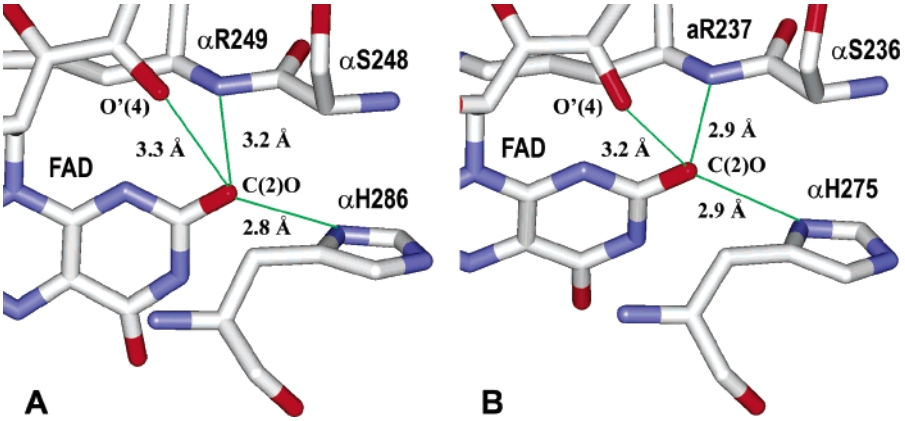

FIGURE 3: Apparent H-bond network on the C(2)O of the FAD in hETF and wETF. A: hETF (PDB code, 1EFV). B: (wETF) (PDB code, 1O97). Both (A) and (B) are shown with similar view angles. Color code: gray, carbon; red, oxygen; blue, nitrogen. Note that only a portion of the FAD cofactor and the relevant amino acid residues are shown for greater clarity.

isoalloxazine ring, an interaction that plays a crucial role in the control of the properties of the flavin (*33*, *34*). However, the assignments of N(5) relevant Raman bands are not as exclusive and specific as for the carbonyl bands. Based on isotopic substitution studies and theoretical calculations (*9*−*14*), the stretching modes for N(5)═C(4a) and N(1)═C(10a) are often coupled and make dominant contributions to Raman bands II and III (*9*−*11*). Band II shifts to higher frequencies when hydrogen-bonding potential is added to N(5) during the calculation (*11*). Various theoretical vibration mode analyses suggest that band II also contains minor contributions from N(10)−C(10a) or N(10)−C(9a) stretching vibrations, while band III does not contain any N(10) relevant information (*9*, *10*, *14*). More recent density functional theory calculations suggest that band III contains contributions from N(1)═C(10a) in addition to C−C stretching modes in ring I (*12*−*14*). Band IV may be linked to both the N(5)═C(4a)/N(1)═C(10a) and ring I C−C stretching modes (*12*−*14*). Yet, isotopic substitution studies involving the N(5) atom only induced significant shifts in bands II and III (*11*). By comparing the Raman data and crystal structures, Tegoni et al. (*19*) found a correlation between the higher frequencies for both bands II and III and stronger hydrogen-bonding interactions at N(1), N(5), or both, suggesting that both bands contain similar vibration components, the stretching modes relevant to N(1)/N(5). However, they suggest that the sensitivity of band II to hydrogen bonding at N(1)/N(5) depends also on the conformation of the flavin isoalloxazine ring. This conclusion is based on an apparent linear correlation between bands II and III, but only for the flavin ring displaying planar ring conformations ((*19*) and Figure 4). For those flavoproteins with nonplanar flavin conformation, the deviation from the linear correlation may reveal the fact that the band II also contains N(10) relevant information (see discussion below).

The unique structural features of wETF make it a good system for evaluating the specific effects on the relevant Raman bands of changes in the interactions at N(5). According to the crystal structure of wETF, the N(5) appears to be H-bonded only with the side-chain hydroxyl group of αSer254. In contrast, the N(1) has no hydrogen-bonding interaction with the protein but, instead, makes an unusual intramolecular hydrogen-bonding interaction with the O′ (4) hydroxyl group of ribityl side chain of the FAD cofactor (*7*). These interactions are conserved in other members of

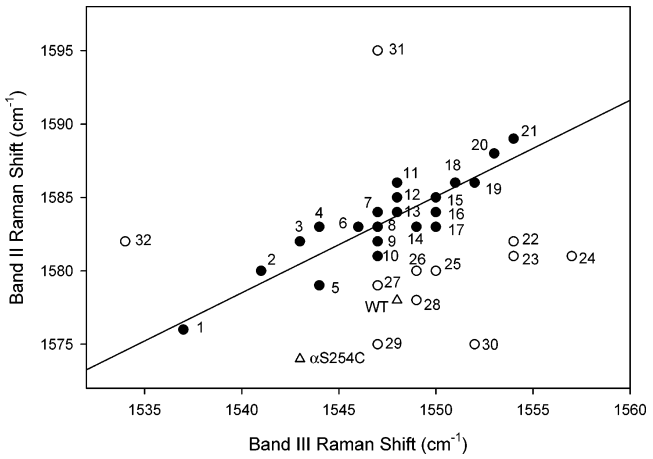

FIGURE 4: Correlations between band II and band III of oxidized flavoproteins. ●, flavoproteins with planar flavin conformation; ○, flavoproteins with nonplanar flavin conformation; △, wETF data. Data points 1, 2, 4, 7, 8, 12, 14−16, 19, 20, 22, 24, and 30−32 were taken from the survey of Tegoni et al. (*19*) with the others as indicated. The numbered points correspond to data for the following samples: 1, cytochrome P450 reductase; 2, glutathione reductase; 3, the complex of D-amino acid oxidase with o-aminobenzoate (*24*); 4, fatty acyl-CoA dehydrogenase; 5, *Desulfovibrio vulgaris* flavodoxin (*45*); 6, Brewer's yeast old yellow enzyme (*24*); 7, chicken egg white riboflavin binding protein; 8, D-amino acid oxidase; 9, the complex of isovalery acyl-CoA dehydrogenase with acetoacetyl-CoA (*24*) and also FAD (unbound) (this work) (overlapping data); 10, *C. beijerinkcii* flavodoxin (*45*); 11, Baker's yeast old yellow enzyme (*45*); 12, old yellow enzyme; 13, chicken egg white riboflavin binding protein (*25*); 14, medium-chain acyl-CoA dehydrogenase; 15, riboflavin, flavin mononucleotide, FAD; 16, butyryl CoA dehydrogenase; 17, chicken riboflavin binding protein (*45*); 18, short-chain acyl-CoA dehydrogenase (*24*); 19, fatty acyl-CoA oxidase; 20, L-lactate monooxygenase ; 21, medium-chain acyl-CoA dehydrogenase (*24*); 22, luciferase; 23, *Aspergillus niger* glucose oxidase (*24*); 24, flavocytochrome b2; 25, choline oxidase (*45*); 26, glucose oxidase (*45*); 27, monomeric sarcosine oxidase (*45*); 28, phenol hydroxylase (*45*); 29, cholesterol oxidase (*45*); 30, flavodoxin; 31, *p*-hydroxybenzoate hydroxylase; 32, *A. niger* glucose oxidase.

ETF family for which crystal structures are available, i.e., hETF (*29*, *35*) and pETF (*36*). The structurally conservative replacement of αSer254 by a cysteine residue should introduce a weaker H-bond on N(5) due to the less polarized SH group and provide a more direct means of evaluating hydrogen-bonding strength on the Raman spectrum. Because of their location on a surface loop, mutations involving

αThr266 of hETF (*37*) and αThr244 of pETF (*38*), the homologues of αSer254 in wETF, are known not to induce any significant global structural changes on the proteins. The αSer254 to cysteine replacement had no apparent effect on the interactions at N(3) of the flavin, because significant differences were not observed for Raman bands X and XIII in the 1100−1300 cm^{-1} region, which contain contributions from the N(3)−H vibration (*11*, *14*). Thus, the direct effects of the amino acid replacement on the flavin ring that are described below can be confidently localized to N(5) interactions.

The replacement of αSer254 with cysteine resulted in the shifting of bands II, III, and IV to lower frequencies, by 3−5 cm^{-1} relative to that of the wild-type wETF (Table 1). Our results are consistent with the previous survey of experimental observations (*19*) and theoretical calculations (*9*−*11*, *14*) that these bands contain contributions from N(5)/N(1) stretching vibrations. When the frequencies obtained for bands II and III for wETF in this study were included with the published data for other flavoproteins in Figure 4, the Raman data for both the wild-type and αS254C mutant of wETF clearly deviate from this linear relationship. If the conclusions of Tegoni et al. (*19*) hold true, this observation suggests that the isoalloxazine ring is nonplanar in these proteins. Yet, the crystal structures of the wild-type wETF and hETF holoproteins indicate that the FAD ring is in a planar configuration in both cases. However, at the high resolution of the wETF structure (PDB 1O97; resolution, 1.60 Å), it is apparent that the N(10)−C′ (1) bond protrudes out from the plane of the isoalloxazine ring in the direction of the *si*-face with a torsion angle of ∼30°. A similar situation is observed in the crystal structure of the hETF (PDB, 1EFV) although the resolution of this structure is somewhat lower (2.10 Å). The N(10) should have a high level of sp^3 hybridization in this configuration. In fact, the chemical shift value for the $^{15}N(10)$ for hETF is among the lowest of all other flavoproteins investigated, a characteristic of a high sp^3 hybridization level and a decreased planarity of the bond orbital on this atom (*8*). As a result, the diminished participation of the lone electron pair on the N(10) in the π-system of the flavin isoalloxazine ring should affect the vibrational frequency of N(10)−C(10a) and N(10)−C(9a) stretching modes. In this way, the frequency of band II is sensitive to the hybridization state of N(10) as well as hydrogen bonding at N(1) or N(5) while band III is sensitive only to the hydrogen bonding. Therefore, within a relatively fixed structural framework, our results provide evidence that the origin of the deviation from linear relationship between the frequencies of bands II and III is more a function of the sp^3 character of the N(10) of the flavin rather than exclusively an indication of the nonplanarity of the whole isoalloxazine ring. Because of its sensitivity to conformation and the mixture of N(5) and N(1) stretching modes, caution must be exercised in the use of frequency shifts for band II in the comparison of presence and strength of hydrogen-bonding interactions at the N(5) position in different flavins or flavoproteins. However, band III may serve as a useful marker in applications utilizing site-directed mutagenesis to introduce conservative amino acid replacements within a protein as demonstrated here for the αS254C mutant of the wETF.

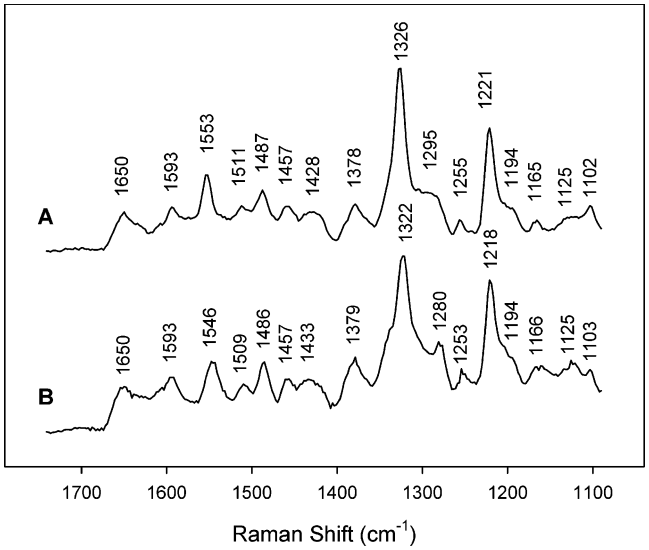

FIGURE 5: Raman spectra of the anionic SQ state of wild-type wETF (A) and the αS254C mutant (B**)** in 50 mM phosphate buffer, pH 7.2, 25 °C.

Raman Spectroscopy of the Anionic SQ Form of wETF and the Spectral Effects of the N(5) Hydrogen-Bonding Interaction. The SQ form of the flavin often serves as a crucial intermediate in flavoprotein-catalyzed redox reactions, yet structural issues involving this redox state are difficult to study by NMR spectroscopy or X-ray crystallography because of its paramagnetic properties, reactivity with oxygen, and intrinsic instability. However, by coupling the advantages of the nonresonance Raman approach with the unusual stability of the SQ^- form of the wETF, good-quality Raman spectra were acquired for the SQ^- form of this protein without the addition of stabilizing ligands or unusual solution conditions. Also, these spectra could be obtained under conditions similar to those used for the acquisition of Raman data for the oxidized state, which aids in the comparison of the two redox states within the same protein. The resulting Raman band frequencies are in general qualitative agreement with the previously reported resonance Raman spectra for the free or bound flavins in their SQ^- state (*16*−*20*) (Figure 5). However, the Raman spectra obtained in this study reveal a more comprehensive band set (Table 2). The Raman band frequencies and intensities observed here for the flavin SQ^- are clearly distinguishable from those of the oxidized flavin (Figure 1). The intensity of the strongest band for the flavin SQ^- (1326 cm^{-1}) was approximately one-third that of the most intense band for the oxidized flavin (at 1352 cm^{-1}) when normalized for concentration.

As was the case for the oxidized state, the generation of the αS254C mutant of wETF provided an opportunity to observe the spectral effects associated with changes in the hydrogen-bonding interaction at the N(5) position of the flavin SQ^-. The binding energy for the SQ^- form of FAD to the αS254C mutant, as estimated from the dissociation constant for the OX state together with the midpoint potential of the ox/sq couple, was reduced by ∼20 kJ/mol relative to wild type (*39*), which is consistent with a weaker hydrogen-bonding interaction at the N(5) of the SQ^- form in the mutant. The αSer254 to cysteine replacement resulted in frequency shifts of ≥4 cm^{-1} in the bands at 1553, 1428, 1326, and 1295 cm^{-1} (Figure 5B and Table 2).

Table 2: Observed Frequencies (cm^{-1}) of Raman Bands of the SQ^- Forms of Seven Various Bound and Free Flavins[a] and the wETF Wild-Type and αS254C Mutant[b]

							wETF		
DAO	MAO	GO	RF	FMN	FCB	LMO	wild type	mutant	shift
		1623					1650	1650	0
1602	1589	1578	1610	1609	1603	1607	1593	1593	0
1555	1549	1553	1558	1562	1558	1563	1553	1546	−7
1516	1518	1514	1498	1523	1527	1506	1511	1509	−2
					1500		1487	1486	−1
1448	1457	1451	1460	1461	1462	1462	1457	1457	0
1422			1425		1419	1420	1428	1433	5
1361	1360				1375	1379	1378	1379	1
1331	1335	1328	1334		1348	1345	1326	1322	−4
1292	1288	1288	1292		1295	1301	1295	1280	−15
	1267	1270				1279	1255	1253	−2
	1242								
1217	1211		1235				1221	1220	−1
1188	1181						1194	1194	0
							1165	1166	1
							1125	1125	0
							1102	1103	1

[a] From: D-amino acid oxidase (DAO) (*16*), monoamine oxidase (MAO) (*20*), glucose oxidase (GO) (*20*), riboflavin (RF) (*18*), FMN (*17*), flavocytochrome b2 (FCB) (*19*), L-lactate monooxyenase (LMO) (*19*). [b] This work.

The band at 1553 cm^{-1} shifts downward by 7 cm^{-1} in the αS254C mutant. The assignment of this band is not as firmly established. The corresponding band in the SQ^- form of D-amino acid oxidase (DAO) (∼1555 cm^{-1}) has been reported to be relatively insensitive to isotopic substitutions at N(5) or any atoms in rings II and III, but this band shifts upward by 4 cm^{-1} during H/D exchange (*16*). The only exchangeable proton in the SQ^- is the N(3)H. Time-resolved resonance Raman studies of the anionic and neutral SQ forms of riboflavin indicate that the frequency of this band shifts to lower frequencies by as much as 16 cm^{-1} upon protonation of the N(5) (from 1558 to 1542 cm^{-1}), which has been attributed to a contribution of C(4a)−C(10a) stretching to this band (*18*). So, while this band shifts significantly in response to the mutation, it may contain several coupled modes. As a result, it may serve as a less reliable marker for changes in N(5) interactions.

The apparent shift in the band at 1428 cm^{-1} may not be of significance due to the broadness of the band. The bands at 1295 and 1326 cm^{-1} in wETF are shifted to lower frequencies (by 15 and 4 cm^{-1}, respectively) in the αS254C mutant. Their counterparts in the spectra for DAO (1292 and 1331 cm^{-1}, respectively), were both affected substantially by isotopic substitutions for the C(4a) or N(5) atoms (*16*). Tegoni et al. (*19*) have compared the Raman spectra of the SQ^- state of DAO, glucose oxidase, and L-lactate monooxygenase and the crystal structures of these proteins in the oxidized state. A correlation was apparent between the hydrogen bonding at the N(5) and N(1) positions and the frequencies of the Raman bands at about 1285 and 1330 cm^{-1}. These results provide strong support for the interpretation that both bands contain significant contributions from N(5)−C(4a) stretching modes. Our results are consistent with these observations and indicate that these two bands can be used effectively as reference markers for monitoring the strength of the hydrogen-bonding interactions at the N(5) in SQ^- form of flavoproteins.

αS254C Mutation-Induced Environmental Changes near the FAD Isoalloxazine Ring in wETF Implied by Raman Data. One of the most significant differences between the Raman spectra of the wild-type wETF and unbound FAD is the large increase in the frequencies of bands I and V, which shift from 1629 and 1464 cm^{-1} for FAD to 1608 and 1450 cm^{-1} for wETF, respectively. Band I is assigned to the stretching vibrations in ring I (the *o*-xylene ring) while band V is primarily associated with C−C stretching in ring I as well as the deformation of two methyl groups (*9*−*14*). As a result, band V is highly sensitive to chemical modifications at positions 7 and 8 of the isoalloxazine ring (*40*, *41*). The frequencies for bands I and V for wild-type wETF are also much lower than most free or bound flavins investigated thus far. Only the nonfluorescent flavoprotein from *Photobacterium leiognathi*, a homologue of bacterial luciferase (*42*), displays comparable values (1603 and 1449 cm^{-1}, respectively) (*23*), which may be the result of the unique covalent modification of C(6) on ring I with the fatty acid myristate (*42*). However, the shifts cannot be accounted for in this way for the FAD bound to wETF. Furthermore, the frequencies of bands I and V were also observed to shift from 1608 and 1450 cm^{-1} in the wild-type wETF to 1622 and 1462 cm^{-1}, respectively, in response to the αSer254 to cysteine replacement, values similar to those of unbound FAD and most other flavoproteins (Figure 2 inset). Because these bands do not contain contributions from N(5)-relevant normal modes, the observed shifts for the αS254C mutant were unexpected. What are these observations signaling about the environment of the FAD in wETF?

Using Raman spectroscopy to monitor the substrate-induced environmental changes to the flavin cofactor in *p*-hydroxybenzoate hydroxylase, Zheng et al. (*14*) have observed that both bands I and V are highly sensitive to the environment of ring I and shift to higher frequencies in a high dielectric environment. Thus, the significant changes in these bands in wETF may be reflecting a change in the environment of ring I in response to this amino acid replacement. While the exact nature of this change is not known, we offer the following possibility based on the comparisons of the crystal structures of wETF (*7*), hETF (*29*), and pETF (*36*) and the current dynamic model of conformational sampling by ETF (*43*). The ETF proteins are heterodimeric and are folded into three distinct domains with the α subunit making up domains I and II and the β subunit comprising domain III. The two methyl groups of ring I are found at the interface between the FAD domain (domain II) and domain III. The former is attached to the rest of the protein (domains I and III) by two flexible loops that seem to serve as a "hinge" (*7*, *44*). Thus, the FAD domain displays an apparent high degree of mobility relative to the rest of the structure. This mobility may be essential for efficient electron transfer from trimethylamine dehydrogenase to wETF (*7*). Based on structural comparisons of the hETF and wETF, Toogood et al. have recently proposed that uncomplexed ETF exists in solution as two interconverting conformational states—one represented by the crystal structure of hETF (designated conformational state I) and the other (designated state II) as represented by the crystal structure of wETF with the FAD domain rotated by ∼40° relative to state I (*43*). This apparent movement of the FAD domain between these two states can result in significant changes in

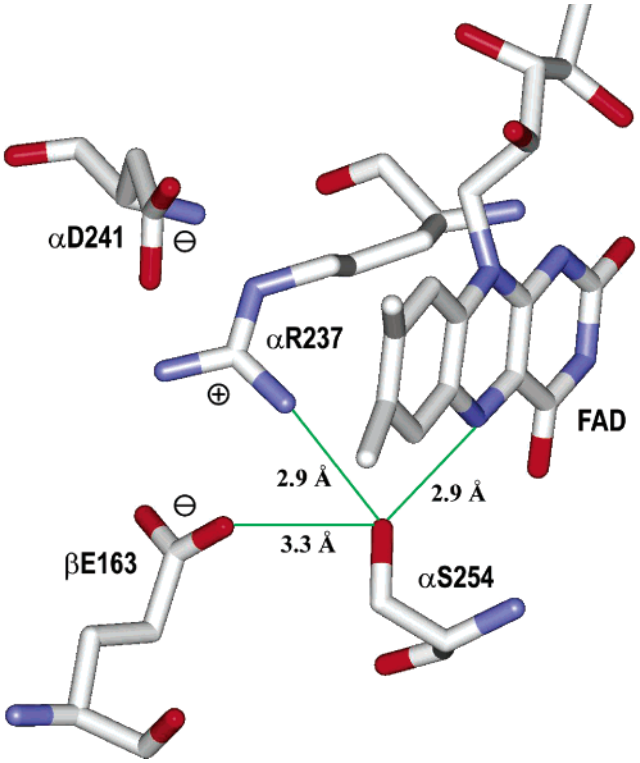

FIGURE 6: Interactions involving αSer254 and associated local interdomain electrostatic interactions in wETF (PDB code, 1O97). The side chain of αSer254 is within hydrogen-bonding distance of the N(5) atom of the FAD cofactor and also with αArg237 and *β*Glu163 (center-to-center distances are shown in angstroms). Interactions between the guanidium group of αArg237 and the side chains of αSer254 and αAsp241 may assist in maintaining the interdomain electrostatic interaction with *β*Glu163. Atom color codes: light gray, carbon; blue, nitrogen; red, oxygen.

the environment of the ring I of the FAD. The amino acid residue αArg249 (corresponding to αArg237 in wETF) in the FAD domain of hETF appears to play a critical role in this conformational transition. In state I, αArg249 is close to *β*Leu185 (hETF numbering). However, in state II, the side chain of this arginine forms an interdomain ion pair with an acidic residue in domain III (*β*Glu165 in hETF or *β*Glu163 in wETF). In wETF, the αArg237 would seem to be restricted to its functional location by the opposing interactions of the guanidine group of αArg237 with the side chains of αSer254 (H-bond) and αD241 (electrostatic interaction) (Figure 6). When αSer254 is replaced by a cysteine residue, the weaker H-bond with αArg237 may cause a change in its location, resulting in the destabilization of state II. As a result, the large shifts in bands I and V in response to the αS254C mutation may be signaling a role of this residue in the dynamics of the FAD domain movement. The relocation of αArg237 induced by the αS254C mutation is also supported by the observation that the C(2)═O band in the αS254C mutant was significantly shifted relative to that of wild type. (Recall that the C(2)O is within hydrogen-bonding distance to the backbone amide group of αArg237.) Therefore, both αArg237 and αSer254, residues that are conserved among the ETF family, appear to be playing crucial interrelated roles in the electron-transfer mechanism of these proteins.

Conclusions. Nonresonance Raman spectroscopy has been used to investigate several protein−flavin interactions in both the oxidized and the SQ^- states of the flavin cofactor within the same flavoprotein. Through site-directed mutagenesis, the spectral changes associated with alterations in the hydrogen-bonding interactions at the N(5) of the FAD in both oxidation states have been established. Several unique structural features of wETF were established from the Raman data of the oxidized protein. In contrast to what is suggested by the crystal structure, the hydrogen-bonding interactions at C(4)O in wETF appear to be very weak or nonexistent. However, by the criteria established by the Raman data, the C(2)O is strongly H-bonded to the protein, which should affect the chemical characteristics of the cofactor. The Raman data support the observation from the crystal structure that the N(10) of flavin in wETF has a high level of sp^3 hybridization, which seldom occurs in oxidized flavins. The αS254C mutation induced shifts in specific N(5)-relevant Raman bands in both redox states of the wETF, demonstrating their sensitivity to N(5) H-bond and establishing specific Raman markers for this interaction. Band III, which has a frequency of ∼1548 cm^{-1} in the oxidized flavin, appears to be a more reliable marker than band II to monitor this interaction. Bands at about 1295 and 1326 cm^{-1} would appear to be useful Raman markers for the N(5) interactions in the flavin SQ^- form. Finally, the ring I-relevant bands in wETF display unusually low frequencies, which suggests that this ring is found in a microenvironment different from that of other flavoproteins. The αS254C mutation affected these bands suggesting that the environment of ring I is altered, perhaps as the consequence of changes in the mobility of the FAD domain of wETF. While our Raman data indicate that the wETF shares some of the structural properties similar to those of the hETF, quantitative differences may be associated with differences in the observed biochemical properties exhibited by these two proteins, such as their redox potentials and redox behaviors.

ACKNOWLEDGMENT

Nonresonance Raman spectra were obtained in Dr. Paul Carey's laboratory at Case West Reserve University. We are also grateful for the technical support from Drs. Jian Dong and Yuangang Zheng during the acquisition of the Raman data.

REFERENCES

1. Thorpe, C. (1991) Electron-transferring flavoproteins, in *Chemistry and Biochemistry of Flavoenzymes*, pp 471−86, CRC Press, Boca Raton, FL.
2. O'Neill, H., Mayhew, S. G., and Butler, G. (1998) Cloning and analysis of the genes for a novel electron-transferring flavoprotein from Megasphaera elsdenii. Expression and characterization of the recombinant protein, *J. Biol. Chem. 273*, 21015−24.
3. Tsai, M. H., and Saier, M. H., Jr. (1995) Phylogenetic characterization of the ubiquitous electron transfer flavoprotein families ETF-alpha and ETF-beta, *Res. Microbiol. 146*, 397−404.
4. Loehr, J. P., Goodman, S. I., and Frerman, F. E. (1990) Glutaric acidemia type II: heterogeneity of clinical and biochemical phenotypes, *Pediatr. Res. 27*, 311−5.
5. Davidson, V. L., Husain, M., and Neher, J. W. (1986) Electron transfer flavoprotein from Methylophilus methylotrophus: properties, comparison with other electron transfer flavoproteins, and regulation of expression by carbon source, *J. Bacteriol. 166*, 812−7.
6. Byron, C. M., Stankovich, M. T., Husain, M., and Davidson, V. L. (1989) Unusual redox properties of electron-transfer flavoprotein from Methylophilus methylotrophus, *Biochemistry 28*, 8582−7.

7. Leys, D., Basran, J., Talfournier, F., Sutcliffe, M. J., and Scrutton, N. S. (2003) Extensive conformational sampling in a ternary electron transfer complex, *Nat. Struct. Biol. 10*, 219−25.
8. Griffin, K. J., Degala, G. D., Eisenreich, W., Muller, F., Bacher, A., and Frerman, F. E. (1998) ^{31}P-NMR spectroscopy of human and Paracoccus denitrificans electron transfer flavoproteins, and ^{13}C- and ^{15}N-NMR spectroscopy of human electron transfer flavoprotein in the oxidised and reduced states, *Eur. J. Biochem. 255*, 125−32.
9. Bowman, W. D., and Spiro, T. G. (1981) Normal mode analysis of lumiflavin and interpretation of resonance Raman spectra of flavoproteins, *Biochemistry 20*, 3313−8.
10. Abe, M., and Kyogoku, Y. (1987) Vibrational analysis of flavin derivatives-normal coordinate treatments of lumiflavin, *Spectrochim. Acta 43A*, 1027−37.
11. Lively, C. R., and McFarland, J. T. (1990) Assignment and the effect of hydrogen bonding on the vibrational normal modes of flavins and flavoproteins, *J. Phys. Chem. 94*, 3980−94.
12. Wille, G., Ritter, M., Friedemann, R., Mantele, W., and Hubner, G. (2003) Redox-triggered FTIR difference spectra of FAD in aqueous solution and bound to flavoproteins, *Biochemistry 42*, 14814−21.
13. Unno, M., Sano, R., Masuda, S., Ono, T., and Yamauchi, S. (2005) Light-induced structural changes in the active site of the BLUF domain in AppA by raman spectroscopy, *J. Phys. Chem. B 109*, 12620−6.
14. Zheng, Y., Dong, J., Palfey, B. A., and Carey, P. R. (1999) Using Raman spectroscopy to monitor the solvent-exposed and "buried" forms of flavin in *p*-hydroxybenzoate hydroxylase, *Biochemistry 38*, 16727−32.
15. Nozaki, D., Iwata, T., Ishikawa, T., Todo, T., Tokutomi, S., and Kandori, H. (2004) Role of Gln1029 in the photoactivation processes of the LOV2 domain in adiantum phytochrome3, *Biochemistry 43*, 8373−9.
16. Nishina, Y., Tojo, H., and Shiga, K. (1988) Resonance Raman spectra of anionic semiquinoid form of a flavoenzyme, D-amino acid oxidase, *J. Biochem. (Tokyo) 104*, 227−31.
17. Sakai, M., and Takahashi, H. (1996) One-electron photoreduction of flavin mononucleotide: Time-resolved resonance Raman and absorption study, *J. Mol. Struct. 379*, 9−18.
18. Su, Y., and Tripathi, G. N. R. (1994) Time-resolved resonance Raman observation of protein-free riboflavin semiquinone radicals, *J. Am. Chem. Soc. 116*, 4405−7.
19. Tegoni, M., Gervais, M., and Desbois, A. (1997) Resonance Raman study on the oxidized and anionic semiquinone forms of flavocytochrome b2 and L-lactate monooxygenase. Influence of the structure and environment of the isoalloxazine ring on the flavin function, *Biochemistry 36*, 8932−46.
20. Yue, K. T., Bhattacharyya, A. K., Zhelyaskov, V. R., and Edmondson, D. E. (1993) Resonance Raman spectroscopic evidence for an anionic flavin semiquinone in bovine liver monoamine oxidase, *Arch. Biochem. Biophys. 300*, 178−85.
21. Altose, M. D., Zheng, Y., Dong, J., Palfey, B. A., and Carey, P. R. (2001) Comparing protein-ligand interactions in solution and single crystals by Raman spectroscopy, *Proc. Natl. Acad. Sci. U.S.A. 98*, 3006−11.
22. Chen, D., and Swenson, R. P. (1994) Cloning, sequence analysis, and expression of the genes encoding the two subunits of the methylotrophic bacterium W3A1 electron transfer flavoprotein, *J. Biol. Chem. 269*, 32120−30.
23. Visser, A. J., Vervoort, J., O'Kane, D. J., Lee, J., and Carreira, L. A. (1983) Raman spectra of flavin bound in flavodoxins and in other flavoproteins. Evidence for structural variations in the flavin-binding region, *Eur. J. Biochem. 131*, 639−45.
24. Hazekawa, I., Nishina, Y., Sato, K., Shichiri, M., Miura, R., and Shiga, K. (1997) A Raman study on the C(4)=O stretching mode of flavins in flavoenzymes: hydrogen bonding at the C(4)=O moiety, *J. Biochem. (Tokyo) 121*, 1147−54.
25. Kim, M., and Carey, P. R. (1993) Observation of a carbonyl feature for riboflavin bound to riboflavin-binding protein in the red-excited Raman spectrum, *J. Am. Chem. Soc. 115*, 7015−6.
26. Thijs, R., and Zeegers-Huyskens, T. (1984) Infrared and Raman studies of hydrogen-bonded complexes involving acetone, acetophenone and benzophenone. 1. Thermodynamic constants and frequency-shifts of the nu-OH and nu-C=O stretching vibrations, *Spectrochim. Acta 40A*, 307−13.
27. Monaco, H. L. (1997) Crystal structure of chicken riboflavin-binding protein, *Embo. J. 16*, 1475−83.
28. Macheroux, P., Kieweg, V., Massey, V., Soderlind, E., Stenberg, K., and Lindqvist, Y. (1993) Role of tyrosine 129 in the active site of spinach glycolate oxidase, *Eur. J. Biochem. 213*, 1047−54.
29. Roberts, D. L., Frerman, F. E., and Kim, J. J. (1996) Three-dimensional structure of human electron transfer flavoprotein to 2.1-Å resolution, *Proc. Natl. Acad. Sci. U.S.A. 93*, 14355−60.
30. Xu, D., Kohli, R. M., and Massey, V. (1999) The role of threonine 37 in flavin reactivity of the old yellow enzyme, *Proc. Natl. Acad. Sci. U.S.A. 96*, 3556−61.
31. Ghisla, S., and Massey, V. (1986) New flavins for old: artificial flavins as active site probes of flavoproteins, *Biochem. J. 239*, 1−12.
32. Hall, L. H., Bowers, M. L., and Durfor, C. N. (1987) Further consideration of flavin coenzyme biochemistry afforded by geometry-optimized molecular orbital calculations, *Biochemistry 26*, 7401−9.
33. Chang, F. C., and Swenson, R. P. (1999) The midpoint potentials for the oxidized-semiquinone couple for gly57 mutants of the *Clostridium beijerinckii* flavodoxin correlate with changes in the hydrogen-bonding interaction with the proton on N(5) of the reduced flavin mononucleotide cofactor as measured by NMR chemical shift temperature dependencies, *Biochemistry 38*, 7168−76.
34. Kasim, M., and Swenson, R. P. (2001) Alanine-scanning of the 50's loop in the *Clostridium beijerinckii* flavodoxin: evaluation of additivity and the importance of interactions provided by the main chain in the modulation of the oxidation−reduction potentials, *Biochemistry 40*, 13548−55.
35. Dwyer, T. M., Mortl, S., Kemter, K., Bacher, A., Fauq, A., and Frerman, F. E. (1999) The intraflavin hydrogen bond in human electron transfer flavoprotein modulates redox potentials and may participate in electron transfer, *Biochemistry 38*, 9735−45.
36. Roberts, D. L., Salazar, D., Fulmer, J. P., Frerman, F. E., and Kim, J. J. (1999) Crystal structure of *Paracoccus denitrificans* electron transfer flavoprotein: structural and electrostatic analysis of a conserved flavin binding domain, *Biochemistry 38*, 1977−89.
37. Salazar, D., Zhang, L., deGala, G. D., and Frerman, F. E. (1997) Expression and characterization of two pathogenic mutations in human electron transfer flavoprotein, *J. Biol. Chem. 272*, 26425−33.
38. Griffin, K. J., Dwyer, T. M., Manning, M. C., Meyer, J. D., Carpenter, J. F., and Frerman, F. E. (1997) alphaT244M mutation affects the redox, kinetic, and in vitro folding properties of *Paracoccus denitrificans* electron transfer flavoprotein, *Biochemistry 36*, 4194−202.
39. Yang, K.-Y., and Swenson, R. P. (2007) Modulation of the redox properties of the flavin cofactor through the hydrogen-bonding interactions with the N(5) atom: Role of αSer254 in the electron transfer flavoprotein from the methylotrophic bacterium W3A1 *Biochemistry*, *46*, 2289−2297.
40. Schopfer, L. M., Haushalter, J. P., Smith, M., Milad, M., and Morris, M. D. (1981) Resonance Raman spectra for flavin derivatives modified in the 8 position, *Biochemistry 20*, 6734−9.
41. Schopfer, L. M., and Morris, M. D. (1980) Resonance Raman spectra of flavin derivatives containing chemical modifications in positions 7 and 8 of the isoalloxazine ring, *Biochemistry 19*, 4932−5.
42. Moore, S. A., James, M. N., O'Kane, D. J., and Lee, J. (1992) Crystallization of Photobacterium leiognathi non-fluorescent flavoprotein, an unusual flavoprotein with limited sequence identity to bacterial luciferase, *J. Mol. Biol. 224*, 523−6.
43. Toogood, H. S., van Thiel, A., Basran, J., Sutcliffe, M. J., Scrutton, N. S., and Leys, D. (2004) Extensive domain motion and electron transfer in the human electron transferring flavoprotein.medium chain Acyl-CoA dehydrogenase complex, *J. Biol. Chem. 279*, 32904−12.
44. Jones, M., Basran, J., Sutcliffe, M. J., Gunter, Grossmann, J., and Scrutton, N. S. (2000) X-ray scattering studies of Methylophilus methylotrophus (sp. W3A1) electron-transferring flavoprotein. Evidence for multiple conformational states and an induced fit mechanism for assembly with trimethylamine dehydrogenase, *J. Biol. Chem. 275*, 21349−54.
45. Zheng, Y. (2002) Ph.D. Thesis, Case Western Reserve University, Cleveland, OH.

BI061628A